

INVESTIGATION OF THE INHIBITION EFFECT OF 5-MERCAPTO-1-PHENYL-TETRAZOLE AGAINST COPPER CORROSION IN ACIDIC MEDIA

M. Shaglouf, A. Shaban, Gy. Vastag*, E. Szöcs, E. Kálmán

H. A. S., Chemical Research Center, H-1525 Budapest, P.O Box 17,
Hungary.

*University of Novi Sad, Faculty of Natural Sciences and
Mathematics, Trg D. Obradovica 3, 21000 Novi Sad, Serbia and
Montenegro.

ABSTRACT

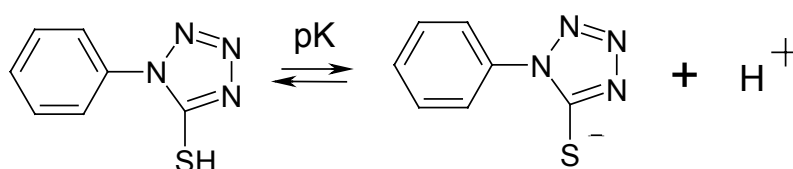
As copper protection is considered to be a very important task in acid media, where corrosion attacks are severe and costly. Surface sensitive techniques such as electrochemical quartz crystal microbalance (EQCM) and electrochemical scanning tunnelling microscopy (EC-STM) were applied to study the potential dependence of adsorption and kinetic properties of inhibitor film formation on copper surface in acidic environment. The investigated inhibitor was 5-mercapto-1-phenyl-tetrazole (5-MPhTT) and the electrolyte solution was 0.1M Na₂SO₄ (pH=2.94). In order to study the electrode mass changes in the absence and presence of the inhibitor at rest potential, QCM investigations were performed. The apparent mass and current variation as a function of the electrode potential was registered in order to study the protective film and its breakdown. Surface morphology and anodic dissolution of Cu(111) electrodes in inhibited and uninhibited electrolytes were studied by in situ STM technique. Information about the nature of the protective layer was given by the STM images. The results were analyzed and discussed.

INTRODUCTION

Several copper corrosion inhibitors have been known and applied for

corrosion protection. Some of these inhibitors such as triazoles, azoles derivatives are not so effective in acidic solutions as in alkaline and neutral environments [1,2,3]. It is well known that effective inhibitors contain N and/or S atoms, due to the ability to easily form bounds with transition metals such as copper [4,5]. Trabanelli and his co-workers reported that, the inhibition effectiveness might be due to the formation of thin layers of copper-inhibitor complexes [6,7].

We have investigated different heterocyclic compounds as copper corrosion inhibitors and evaluating the optimum inhibition efficiency of those derivatives in acidic environment [8,9,10]. From those investigated materials we found that 5-mercapto-1-phenyl-tetrazole (5-MPhTT) was the most effective one. The molecule adsorb probably through the -S- or through coordination with nitrogen from the tetrazole ring [9]. In acidic solution the most probable reaction is the protonation reaction of the 5-MPhTT molecule as it has a pK value of 2.8.



In the past few decades numerous investigations were performed using the traditional electrochemical methods [11,12,13], but recently many research groups try to understand processes taking place at electrode surfaces by using in situ surface sensitive techniques like quartz crystal microbalance (QCM) and scanning probe microscopy (SPM) [14,15,16]. These in situ techniques have produced a better understanding of dissolution/deposition of metals and adsorption of different ions by measuring mass differences in order of nanogram per surface area or visualizing the surface morphological changes in nanometer or even atomic scale. Also an important and extensively studied field was also the influence of organic additives on the copper dissolution/deposition reaction [17,18].

Introducing the high resolution STM technique, many investigations

performed the adsorption/desorption of sulfate/bisulfate ions on copper surface and noticed an ordered/disordered adlayer on the copper single crystal surface [19-23].

Marcus and Strehblow [24-26] proved that the EC-STM is a suitable technique to study the initial stage of passive film formation. Magnussen [27] has investigated the copper corrosion and its inhibition by benzotriazole (BTA) and concluded that the BTA inhibited the step-flow dissolution of copper and pits formed on terraces at more anodic potential. EQCM technique was used by Trabanelli and his co-workers [7] to study the effectiveness of several copper corrosion inhibitors in 0.1 mol.dm^{-3} NaCl solutions. They have found that copper electrode pre-filmed with 5-MPhTT gave the lowest corrosion rate during the measuring time. They have also shown that the mass change (Δm), determined in free corrosion conditions, are useful data but these are not absolute values, as the Δm value is an algebraic sum of different processes like: adsorption of inhibitor, formation of surface film or soluble/insoluble surface compounds. Landolt and his co-workers [28] have shown that the electrosorption of inhibitor molecules is a replacement reaction where the observed mass change is due to the adsorption.

Hepel and co-workers [29] combined the EQCM with quartz crystal immittance technique to determine the corrosion breakdown potential in absence and presence of inhibitor, it was concluded that the high positive corrosion breakdown potential in presence of inhibitor is attributed to the increased film compactness associated with strong later interaction between the inhibitor molecules.

EXPERIMENTAL

Quartz Crystal Microbalance (QCM / EQCM) :

Electrochemical nanobalance (model EQCN-701) and AT-cut quartz crystal with nominal frequency of 10 MHz were used. The crystal was coated on both sides by vacuum deposition with chromium (thickness 15 nm) and gold (thickness 180 nm) layers. The copper was deposited on the gold layer. Pt wire was used as counter electrode and saturated calomel electrode (SCE) was used as reference electrode. The frequency change of the crystal is related to the interfacial mass

change, which is caused by electrochemical reactions taking place at the electrode surface. The surface mass change per unit area ($\mu\text{g}/\text{cm}^2$) is proportional to the change of resonance frequency of the quartz crystal (Δf), according to Sauerbrey equation.

The time dependence QCM measurements were performed at rest potential in three intervals. In the first interval, a freshly deposited copper surface after thoroughly washed with water was immediately contacted with the blank solution. In the second interval the electrolyte was exchanged with inhibitor containing solution, while in the third interval the blank solution was used again. Before each solution change we waited few minutes to stabilize the system, then the mass (frequency) vs. time characteristics were recorded. The corrosion breakdown potentials were evaluated using electrochemical QCM, by recording simultaneous linear potential scan voltammetric (i-E) and piezo-gravimetric (m-E) characteristics. Diluted solutions were used and i-E, m-E characteristics were recorded only after the system stabilized, thus there is no change in visco-elastic properties at the interface during measurement. The scan rate of cyclic voltammetric measurements was 1 mV/s. The potentials were swept from -300 mV and reversed at +400 mV back to -300 mV vs. SCE. The OCP was measured to be -36 mV vs. SCE in blank solution, in presence of 5-MPhTT the OPC shifted to positive potential value of +36 mV vs. SCE.

Electrochemical Scanning Tunneling Microscopy (EC-STM):

In situ EC-STM experiment was carried out using a PicoStat apparatus (Molecular Imaging). The tunneling tips were made of tungsten and covered with an epoxy layer up to the operational tip to decrease the Faradic current [30]. A three-electrode electrochemical cell was used. The electrochemical potentials of the electrode and tip were independently controlled by a bi-potentiostat. The electrochemical potential of the tip was held in the double layer region where the Faradic current is minimal. Pt wires (99.9%) were used as reference and counter electrodes. Prior to STM experiments electrochemical current-voltage curves of Cu(111) were recorded and the potentials were referred to SCE. The scan rate of CV measurements was 10 mV/s. The images were taken at constant

current mode with tunneling currents from 0.5nA to 1nA.

RESULTS AND DISCUSSION

Gravimetric test (QCM) results:

Figure 1 shows the mass changes vs. time characteristic. During the first interval, the mass decrease is due to copper dissolution. In presence of inhibitor the mass decrease stopped, which means that a protective film formed on the copper surface, as shown in interval II. In Interval III the mass change remained constant, this is an indication that 5-MPhTT was chemically adsorbed and remained on the surface. The inhibitor efficiency was 98%. We could conclude that 5-MPhTT is effective inhibitor even in more acidic solutions.

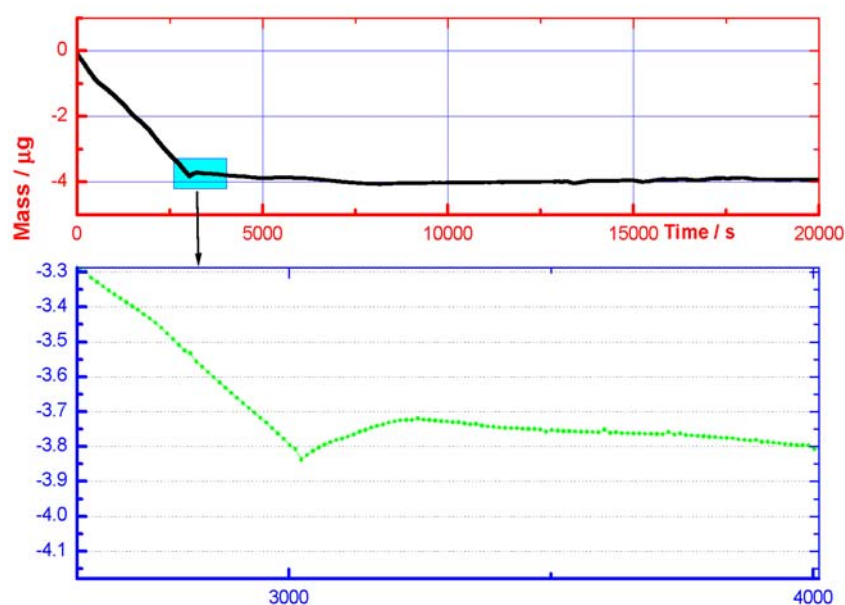


Figure 1. Mass changes in time without and with the addition of inhibitor. I. Interval: Blank solution, II. Interval: 5-MPhTT containing solution, and III. Interval: Blank solution.

EQCM results:

It is clear from table 1 that in the presence of inhibitor the total mass change was twice less than in the blank solution.

Table 1. Breakdown potentials (E_B) and the total mass change (Δm) in blank and inhibitor containing solutions.

| Solutions | E_B (mV/SCE) | Δm_{tot} ($\mu\text{g}/\text{cm}^2$) |
|-----------|----------------|---|
| Blank | -47 | -37.19 |
| 5-MPhTT | 163 | -18.21 |

Figure 2 shows the total mass change and Figure 3 the current density in function of potential. In blank solution, when the anodic current started to flow ($E_B = -47$ mV), the mass loss was approximately continuous. The mass decrease signifying that the predominant process above the breakdown potential is the copper dissolution. The copper dissolution continues up to the anodic reversal potential of +400 mV. On return cathodic going scan further mass decrease is observed. A large reduction peak can be seen on i - E curve but the corresponding mass change is less than the current density demanded.

In presence of 5-MPhTT, copper anodic dissolution started at more positive potential value ($E_B = 163$ mV). The high corrosion breakdown potential indicates the presence of a compact inhibitor film on copper surface [31]. The onset of that small anodic current and mass loss was associated with copper-inhibitor, copper-oxide or salt growth, rather than active copper dissolution. No reduction peak in the reverse cathodic scan direction so that was another attribution that the inhibitor is strongly adsorbed to the surface.

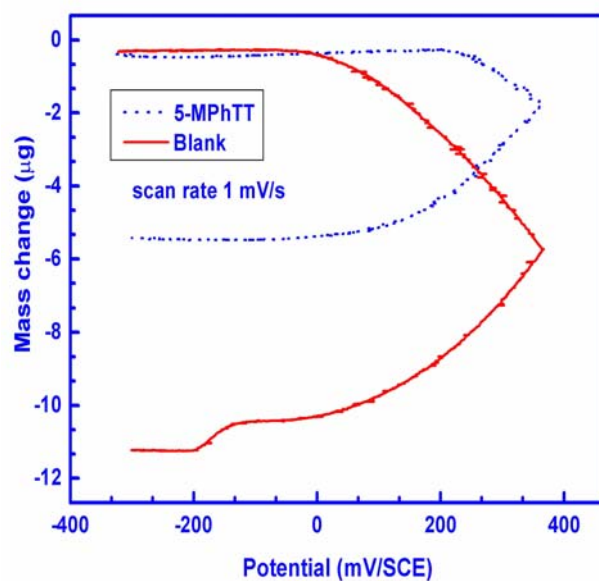


Figure 2. Mass change vs. potential characteristics.

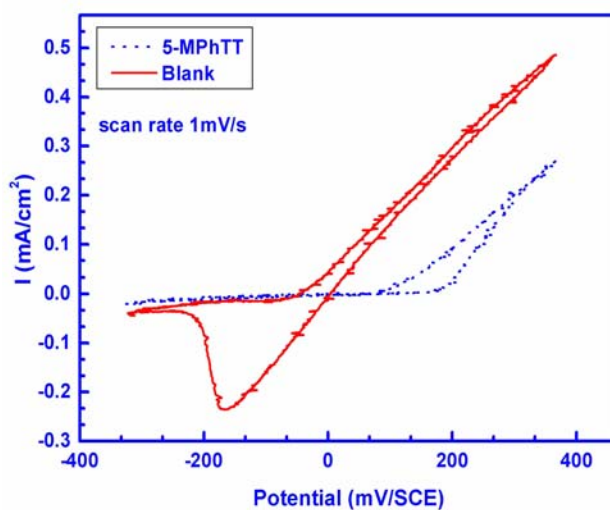


Figure 3. Current-potential characteristics, sweep rate 1 mV/s, solid line represents CV curve recorded in blank solution, dotted line shows the copper behaviour in 5-MPhTT containing solution

EC-STM results:

Fig. 4a. shows the surface morphology at -130 mV where the step edges are frizzy, which is attributed to the presence of sulfate adlayer. It is clear that from Fig. 4b that at -30 mV, the copper dissolution starts via removal of atoms along the step edges. Magnussen did some more detailed investigations about the dissolution of Cu(111) in pure sulfuric acid solution [27] and he also noticed that the copper dissolution starts at step edges and proceeds as a step-flow mechanism.

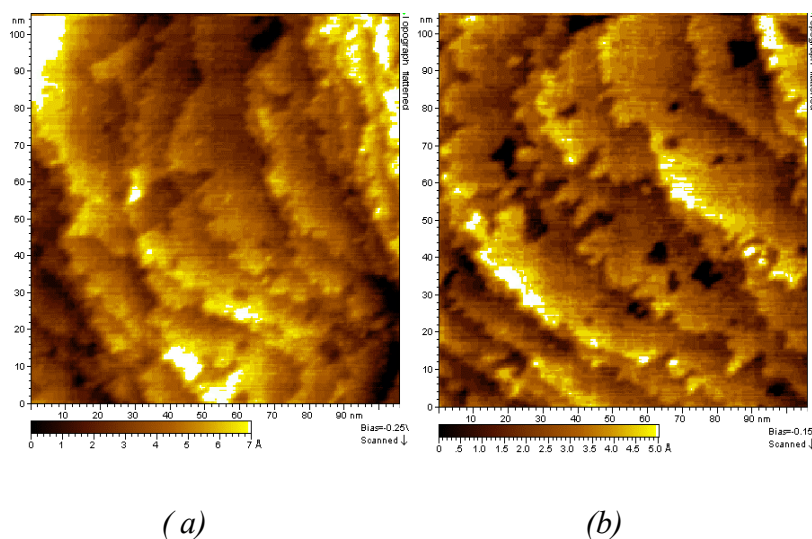
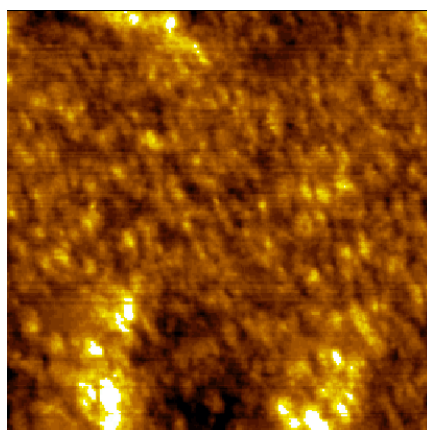


Figure 4.a,b. Series of STM images showing the dissolution of Cu(111) in $1 \text{ mmol.dm}^{-3} \text{ Na}_2\text{SO}_4$ solution (a) Frizzy steps, $E_s = -130$ mV, $U_B = -250$ mV, $I_T = 1$ nA, (b) Dissolution of the step edges, $E_s = -30$ mV, $U_B = -150$ mV, $I_T = 1$ nA, Image size $150 \text{ nm} \times 150 \text{ nm}$.

Figure 5 shows the copper surface in inhibitor containing solution at -70 mV. We observed some small islands on the surface, which size varied between 5-10 nm. These small islands could be inhibitor accumulations.

The dissolution process took place at more positive potential values than in blank solution (Fig 6.a,b,c,d.). At $+120$ mV the image shows the stepped copper surface (Fig. 6a.).

At +220 mV potential the dissolution commences with the formation of small monoatomic pits in the centre of the terraces, the step edges were still visible, but in some places the dissolution has started (Fig. 6b.). At more positive potential value (+320 mV) the size of the pits increases and additional pits nucleate on the terraces (Fig 6c,d.). The surface roughness increases, but there is no significant Cu dissolution at the step edges. This indicates that the steps are strongly stabilized by the 5-MPhTT adlayer and the dissolution starts at places where defect point in the protective layer was.



190 nm x

Figure 5. Surface morphology in $5 \cdot 10^{-4} \text{ mmol.dm}^{-3}$ 5-MPhTT inhibitor concentration, $E_S = -70 \text{ mV}$, $U_B = -200 \text{ mV}$, $I_T = 0.62 \text{ nA}$, Image size 190 nm x 190 nm.

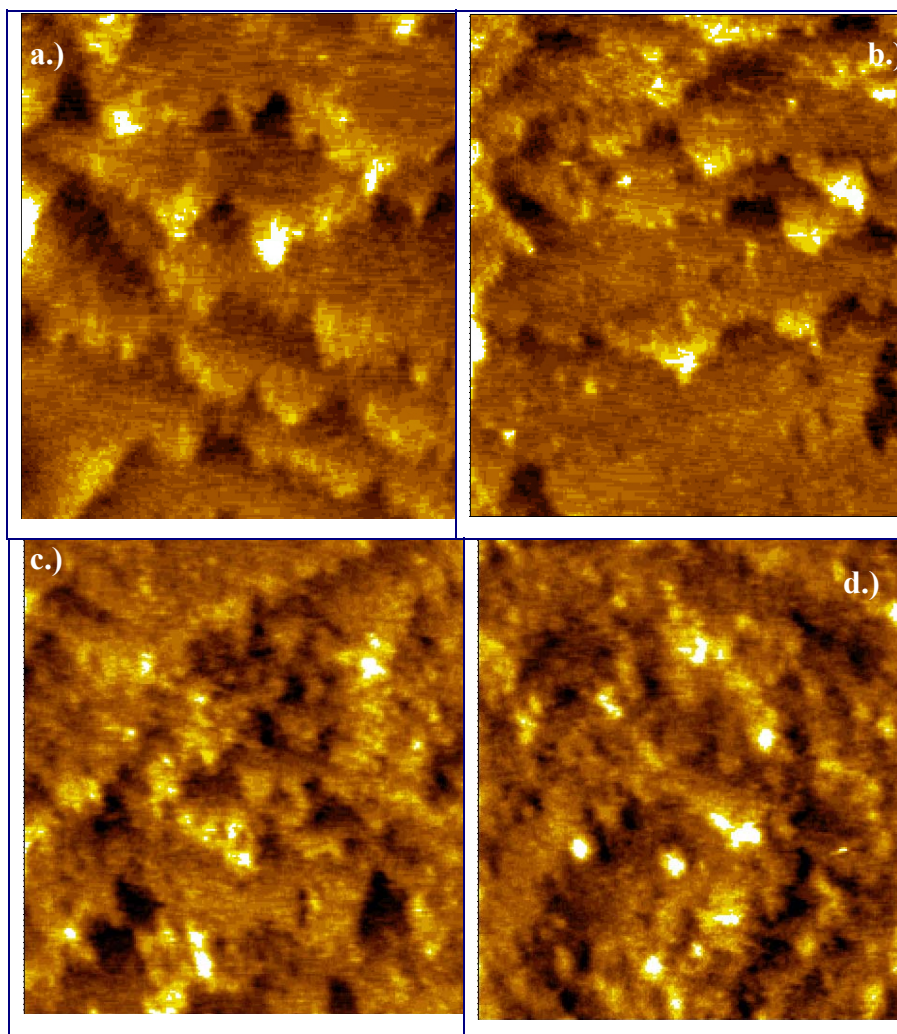


Figure 6.a,b,c,d. Series of STM images showing the copper dissolution in presence of 5-MPhTT, (a) $E_S = +120\text{ mV}$, $U_B = -300\text{ mV}$, $I_T = 1\text{ nA}$, (b) $E_S = +220\text{ mV}$, $U_B = -400\text{ mV}$, $I_T = 1\text{ nA}$, (c) and (d) $E_S = +320\text{ mV}$, $U_B = -250\text{ mV}$, $I_T = 1\text{ nA}$, Image size $85\text{ nm} \times 85\text{ nm}$.

CONCLUSIONS

The results performed from these investigations lead to the following conclusions:

QCM measurements showed that the inhibitor hindered the copper dissolution by forming a protective layer on the copper surface. The inhibitor efficiency reached 98%.

The EQCM results showed that at very slow scan rate (1 mV/s) to anodic potential values, the mass decrease in presence of 5-MPhTT was twice less than in blank solution and the breakdown potential was also more positive in inhibitor containing solution ($E_{\text{Binh}} \gg E_{\text{Bblank}}$). The high corrosion breakdown potential indicated the presence of compact inhibitor film on copper surface.

The adsorption property of 5-MPhTT inhibitor was studied by electrochemical scanning tunneling microscopy. The results showed that in the double-layer potential region an inhibitor layer formed on copper surface, which was removed from the surface at a potential less than -400 mV vs. SCE.

Significant difference was visualized on the copper single crystal dissolution in uninhibited and inhibited sulfuric acid solutions. The copper (Cu(111)) dissolution in sulfuric acid started at the edges of the crystal steps and proceeded along the stairs, the dissolution in presence of 5-mercapto-1-phenyl-tetrazole inhibitor was initiated on terraces because the inhibitor molecules block the step edges.

REFERENCES

1. D.Kuron, H.J.Rother, R.Holm, S.Storp, *Werkstoffe und Korrosion* 37 (1986) 83
2. M.Fleischmann, I.R.Hill, *Electrochim. Acta* 28 (1983) 1325
3. M.Beier, J.W.Schultze, *Electrochim. Acta* 37 (1992) 2299
4. G.Trabanelli, *Corrosion* 47 (6) (1991) 410
5. Shaban, E.Kálmán, J.Telegdi, G.Pálinkás, Gy. Dóra, *Appl. Phys. A66* (1998) 545
6. F.Zucchi, G.Trabanelli, M.Fonsati, *Corrosion Sci.* 38 (1996) 2029
7. M.Fonsati, F.Zucchi, G.Trabanelli, *Electrochim. Acta* 44 (1998) 311
8. Gy.Vastag, E.Szőcs, A.Shaban, I.Bertóti, K.Popov-Pergal, E.Kálmán, *Solid State Ionics* 141-142 (2001) 87
9. Gy.Vastag, E.Szőcs, A.Shaban, E.Kálmán, *Pure Appl. Chem*, 73 (2001) 1861

10. E.Szőcs, Gy.Vastag, A.Shaban, G.Konczos, E.Kálmán, J. Appl. Electrochem 29 (1999) 1339
11. J.B.Cotton, I.R.Scholes, Br.Corros.J. 2 (1967) 1
12. G.W.Poling, Corros.Sci. 10 (1970) 359
13. F.Zucchi, M.Fonsati, G.Trabanelli, Giornate Nazionali Sulla Corrosione e Protezione, 3rd edn, (AIM, Milano, 1996) 115
14. A. Shaban, PhD dissertation, Technical University of Budapest, Budapest (1998)
15. B.J.Cruickshank, A.A.Gewirth, R.M.Rynders, R.Alkire, J. Electrochem. Soc., 139 (1992) 2829
16. M.R.Vogt, A.Lachenwitzer, O.M.Magnussen, R.J.Behm, Surf. Sci., 399 (1998) 49
17. D.Wang, Q.-M.Xu, L.-J.Wan, C.Wang, C.-L.Bai, Langmuir, 18(13) (2002) 5133
18. Sugimasa, L.-J.Wan, J.Inukai, K.Itaya, J. Electrochem. Soc. 149(10) (2002) E367
19. P.Broekmann, M.Wilms, M.Kruft, C.Stuhlmann, K.Wandelt, Surf. Sci., 416 (1998) 121
20. M.Wilms, P.Broekmann, C.Stuhlmann, K.Wandelt, J. Electroanal. Chem., 467(1-2) (1999) 307
21. W.-H.Li, R.J.Nichols, J. Electroanal. Chem., 456 (1998) 153
22. P.Broekmann, M.Wilms, A.Spaenig, K.Wandelt, Progress in Surf. Sci., 67(1-8) (2001) 59
23. O.M.Magnussen, Chem. Rev., 102 (2002) 679
24. V.Maurice, H.-H.Strehblow, P.Marcus, J. Electrochem. Soc. 146 (1999) 524
25. V.Maurice, H.-H.Strehblow, P.Marcus, Surf. Sci. 458 (2000) 185
26. V.Maurice, L.H.Klein, H.-H.Strehblow, P.Marcus, J.Electrochem. Soc. 150 (2003) B316
27. O.M.Magnussen, M.R.Vogt, J.Scherer, R.J.Behm, Appl.Phys.A 66 (1998) 447
28. P.Kern, D.Landolt, J.Electrochem.Soc., 148 (2001) B228
29. M.Hepel, E.Cateforis, Electrochim. Acta, 46 (2001) 3801
30. R.Kazinczi, E.Szőcs, E.Kálmán, P.Nagy, Appl. Phys. A 66 (1998) 535
31. D. Kouznetsov, A. Sugier, F. Ropital, C. Fiaud, Electrochim. Acta, 40 (1995) 1513